NOTATION

a, b = constants, Equation (3)
H° = enthalpy of ideal gas, B.t.u./lb.-mole
H = enthalpy, B.t.u./lb.-mole
P = pressure, lb./sq. in. abs.
R = gas constant
T = absolute temperature, °R.
v = molar volume
z = compressibility factor

Greek Letters

κ = constant, Equation (3)
π = internal pressure, lb./sq. in. abs.

Subscripts

c = critical
T = constant temperature
v = constant volume

LITERATURE CITED

1. Beattie, J. A., and O. C. Bridgeman, *Proc. Am. Acad. Arts Sci.*, **63**, 229 (1928).
2. Benedict, M., G. B. Webb, and L. C. Rubin, *Chem. Eng. Progr.*, **47**, 419 (1951).
3. Hougen, O. A., K. M. Watson, and R. A. Ragatz, "Chemical Process Principles," 2nd edit., Vol. II, Wiley, New York (1959).
4. Thompson, W. H., W. G. Braun, and M. R. Fenske, Documentation of the Basis for Selection of the Contents of Chapter 7, "Technical Data Book-Petroleum Refining," American Petroleum Institute, New York (1966).
5. van der Waals, J. D., dissertation, Leiden (1873).
6. Yesavage, V. F., Ph.D. dissertation, Univ. Michigan, Ann Arbor (1968).

Heat and Mass Transfer for Turbulent Pipe Flow

G. A. HUGHMARK

Ethyl Corporation, Baton Rouge, Louisiana 70821

Heat and mass transfer coefficients for turbulent flow in smooth circular pipes have been represented by empirical equations of the form

$$N_{Nu} = a\,(N_{Re})^b\,(N_{Pr})^c \qquad (1)$$

with various values of the constants a, b, and c to correlate experimental data.

EARLY RESEARCH

The equations of Colburn (*1*), Dittus and Boelter (*2*), Drexel and McAdams (*3*), and Sieder and Tate (*4*) are representative of the significant differences in the constants for Equation (1). These constants represent data for fluids with Prandtl numbers with the approximate range of 1 to 100. Interest in liquid metals as heat transfer media resulted in experimental data which showed that these data for very low Prandtl number fluids could not be predicted by correlations of the form of Equation (1). This difference occurs because the wall region, with characteristics of laminar flow, provides the resistance for heat transfer with Prandtl numbers greater than one, but the fully turbulent core region represents much of the resistance for the liquid metals.

The velocity profile was subdivided by von Karman (*5*) into three regions: laminar, buffer, and turbulent core. The velocity data of Nikuradse (*6*) were used to determine the eddy diffusivity for momentum as a function of the dimensionless radial distance, and an equation was derived to relate the Stanton number to the friction factor and Prandtl number. Martinelli (*7*) extended the concept of von Karman to include the core region and to use the velocity profile to obtain temperature profiles at uniform flux to predict heat transfer coefficients. Martinelli's assumptions were:

1. The "laminar sublayer" corresponds to y^+ from 0 to 5 and $\epsilon_H = 0$.
2. A buffer layer for y^+ from 5 to 30 and $\epsilon_H = \epsilon_v$.
3. The turbulent core for y^+ greater than 30 and $\epsilon_H = \epsilon_v$.

Inclusion of the core region provided the basis for prediction of heat transfer coefficients for liquid metals in addition to the Prandtl number range of 1 to 10 that was adequately represented by the von Karman equation. Experimental data for mass transfer showed that the von Karman equation underestimates the transfer rate because turbulence exists in the laminar sublayer. Lin, Moulton, and Putnam (*8*) recognized this sublayer turbulence and suggested introduction of an eddy of magnitude $\epsilon/\nu = 0.00033\,(y^+)^3$ into the laminar sublayer. Kropholler and Carr (*9*) used this eddy representation with a four-region velocity profile to develop a heat and mass transfer correlation. Equal diffusivities were assumed for momentum,

Correspondence concerning this article should be addressed to Dr. G. A. Hughmark.

heat, and mass.

Hughmark (*10*) extended the velocity profile analysis to include numerical integration of a six region velocity profile with the Marchello and Toor mixing model for thermal and mass diffusivity in the wall region and equal thermal and momentum diffusivity in the core. Numerical integration provided the flexibility to consider the local apparent viscosity as a function of the local shearing stress for non-Newtonian fluids and for the local physical properties as a function of temperature. The purpose of this paper is to utilize recent work to improve this model.

EDDY DIFFUSIVITY IN THE CORE REGION

Many models have been proposed for the relationship of the eddy diffusivities for heat and momentum in the core region, Jenkins (*11*) and Azer and Chao (*12*) have used mixing length models. Deissler (*13*) analyzed turbulent heat transfer and temperature fluctuations in a field with uniform velocity and temperature gradients. He also obtained the eddy diffusivity ratio for heat and mass and showed that the ratio approaches unity at high velocity gradients, regardless of the value of the Prandtl number. Tyldesley and Silver (*14*) proposed a fluid entity model. Goldman and Marchello (*15*) experimentally determined eddy diffusivities for mass with a point source technique and used these data to develop a model of the form

$$\frac{\epsilon_v}{\epsilon_m} = f\left(\frac{\epsilon_v}{\nu},\ N_{Sc}\right) \tag{2}$$

Baldwin and Walsh (*16*) obtained data for air with a line source of heat and showed that the equation

$$\epsilon_H + K = 0.0021\, a\, u_c \tag{3}$$

applied for the experimental range of Reynolds numbers, 280,00 to 640,000. This is consistent with Taylor's (*17*) reasoning by dimensional analysis that the group $\epsilon_H/2u_ca$ should be a function of pipe Reynolds number. Experimental data indicate that the group has a constant value at high Reynolds numbers. Johnk and Hanratty (*17*) reported temperature profile data for air in the Reynolds number range of 18,000 to 71,000 and correlated the core diffusivity data by the equation

$$\epsilon_H + K = 0.081\ a\ u^* \tag{4}$$

Equation (4) is derived with the assumption of constant eddy diffusivity for momentum and heat in the core region.

These models represent a wide range of values for the eddy diffusivity for heat at similar conditions. A comparison of calculated diffusivities shows this range. Such a comparison first requires calculation of the eddy diffusivity for momentum. This is obtained from the velocity profile which appears to be best represented by the Bogue and Metzner (*18*) equation for Newtonian and non-Newtonian fluids

$$u^+ = 5.57 \log_{10} y^+ + 5.57 - c(\xi, f) \tag{5}$$

$$c(\xi, f) = 0.05\sqrt{2/f}\exp\frac{-(\xi - 0.8)^2}{0.15} \tag{6}$$

Johnk and Hanratty assumed that the eddy diffusivity for momentum is constant for the core region. Another model can be derived with the relationship

$$\epsilon_v + \nu = \alpha/r^n \tag{7}$$

for the core region. Thus, the equation for momentum transport is

$$\frac{\tau}{\rho} = \frac{\alpha}{r^n}\frac{du}{dr} \tag{8}$$

With linear variation in shear stress, Equation (8) is integrated to obtain

$$\frac{u - u_c}{u_c} = \frac{\tau_0\, a^{(2+n)}\, g_c}{(2+n)a\,\rho\,\alpha\,u_c}\left(\frac{r}{a}\right)^{2+n} \tag{9}$$

Velocity profiles for the core obtained from Equations (5) and (6) for the Reynolds number range of 10,000 to 70,000 are represented by

$$\frac{u_c - u}{u_c} = 0.29\left(\frac{r}{a}\right)^{1.9} \tag{10}$$

Solution of Equations (7), (9), and (10) results in the equation for the eddy diffusivity for momentum

$$\epsilon_v + \nu = \frac{1.78\, u^{*2}\, a}{u_c}\left(\frac{r}{a}\right)^{0.1} \tag{11}$$

Eddy Diffusivity Ratios

Table 1 shows calculated values of the eddy diffusivity ratio for Prandtl numbers of 0.029 and 14.3 which repre-

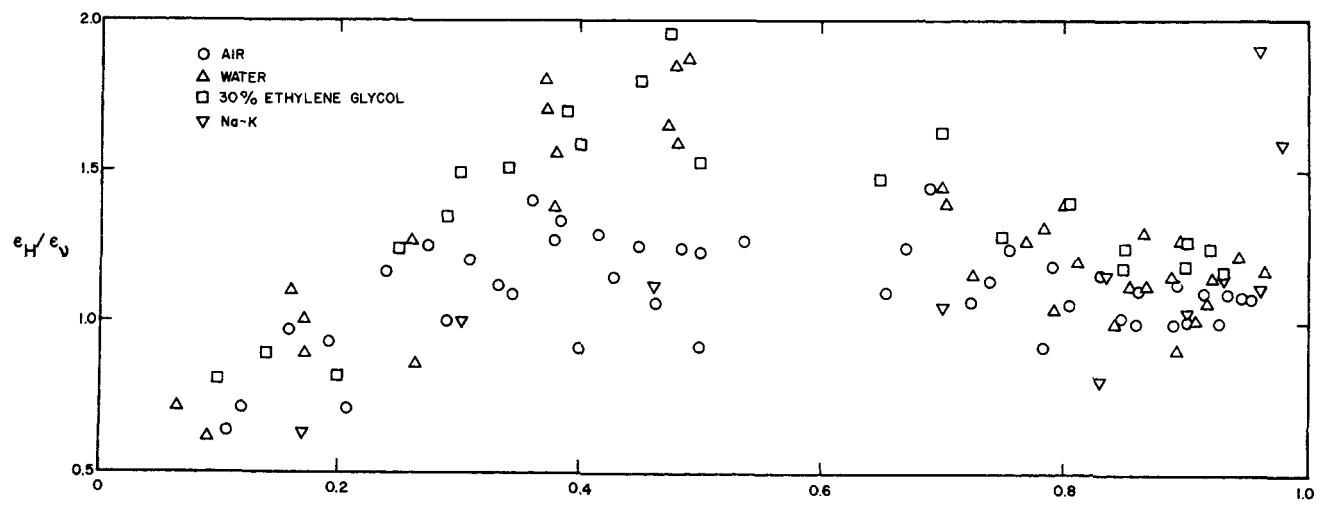

Fig. 1. Eddy diffusivity ratio from temperature profile data.

sents extrapolation for the last three models in the table. A wide range of calculated values are observed for the various models. Experimental temperature profiles have been obtained at constant heat flux for several fluids, which provides a means of determining the eddy diffusivity for heat as a function of radial position in a circular conduit. Such data have been obtained for mercury and alkali metals, but a comparison of the data shows wide differences in the eddy diffusivities for apparently similar conditions. Buhr, Carr, and Balzhiser (*19*) determined temperature profiles for the NaK eutectic and mercury in an attempt to resolve the experimental discrepancies. They concluded that the differences are a result of a distorting free convection effect and that this may occur for mercury at Reynolds numbers of at least 50,000. Their profile data for the NaK eutectic appear to be free of this distortion and are useful in evaluation of the eddy diffusivity for heat.

Other temperature profile data are reported by Johnk and Hanratty for air and by Gowen and Smith (*20*) for water and 30% ethylene glycol in water. Eddy diffusivities for heat have been calculated from these profile data and eddy diffusivities for momentum using the Bogue and Metzner velocity profile equations. The eddy diffusivity ratios obtained in this manner are shown as a function of radial position for all data in which $y^+ > 35$. The liquid metal data appear to be consistent with the higher Prandtl number data. Also with consideration of the error in both diffusivities, it appears that $\epsilon_H/\epsilon_\nu = 1$ is a good assumption. Comparison with Table 1 shows that the Johnk and Hanratty model gives the only values that are consistent with the data shown by Figure 1.

Specific Core Areas

Experimental data for diffusion in the core can be compared with the eddy diffusivity for momentum integrated to represent specific core areas. An integrated value for the eddy diffusivity for momentum was calculated from the velocity profile represented by the Bogue and Metzner equation for a core area with a radius of 25% of the pipe radius. Turbulent Peclet numbers (Du_c/ϵ) calculated from these diffusivities at several Reynolds numbers are shown by Table 2.

Baldwin and Walsh obtained data for the mean temperature profile in air downstream from a line source of heat for diffusion in a core area representing about 25% of the pipe radius. Becker, Rosensweig, and Gwozdz (*21*) analyzed the dispersion of a smoke tracer in air from a point source on the pipe center line and also for a core for 25% of the pipe radius. Towle and Sherwood (*22*) and Flint (*23*) obtained data for the core dispersion of carbon dioxide and hydrogen in air. Mickelson (*24*) reported data for helium in air and Goldman and Marchello (*15*) for helium, carbon dioxide, and *n*-octane in air. Kada (*23*) obtained data for potassium chloride solution in water. Turbulent Peclet numbers from these data are summarized in Table 3.

Table 1. Calculated Values of ϵ_H/ϵ_ν

Reference	Prandtl number 0.029	14.3
Jenkins	1.8	0.7
Azer and Chao	0.43	1.2
Marchello and Toor	0.21	3.6
Tyldesley and Silver	0.12	1.47
Goldman and Marchello	0.034	0.67
Baldwin and Walsh	0.75	0.75
Johnk and Hanratty	1.22	1.2

Table 2. Calculated Turbulent Peclet Numbers

Reynolds number	Turbulent Peclet number
15,000	670
100,000	750
200,000	775
500,000	780

Problems Encountered

Disturbance of the flow by the source and detection device and the contribution of molecular diffusivity are problems encountered in obtaining these experimental data. Becker, Rosensweig, and Gwozdz minimized flow disturbance and used submicron size oil droplets as the diffusing material with a negligible molecular diffusivity. As shown in Table 2, these data represent a Reynolds number region in which the field of turbulence is nearly homogeneous and isotropic. The Baldwin and Walsh data also represent a Reynolds number with a nearly homogeneous and isotropic field of turbulence and a relatively high eddy diffusivity in comparison to the molecular thermal diffusivity. These data are in reasonable agreement with the Becker et al. data. The other data show variations in the turbulent Peclet number which may be a result of flow disturbance, assumption of additive molecular and eddy diffusivities for dispersion in the core, or lack of a homogeneous and isotropic field which is indicated by Table 2 for the lower Reynolds numbers. Thus, eddy diffusivities calculated from the Bogue and Metzner equation are about 10% less than the best experimental data for the core region.

EDDY DIFFUSIVITY IN THE WALL REGION

Hughmark (*25*) analyzed heat and mass transfer in the wall region. The conclusion from this work is that an eddy diffusivity model and a parallel conductance model appear to represent heat and mass transfer data. The eddy diffusivity model is also shown to be derived for developing flow in the laminar sublayer. Sirkar and Hanratty (*26*) recently reported experimental data for the transverse shear stress fluctuations in the wall region which indicate:

$$\frac{n\nu}{u^{*2}} = 9.1 \times 10^{-3} \qquad (12)$$

Popovich and Hummel (*27*) observed that the most probable thickness for the laminar sublayer in turbulent pipe flow is $y^+ = 4.3$ and that turbulence always exists beyond $y^+ = 34.6$. Their observations, together with the recent data by Sirkar and Hanratty, suggest a re-evaluation of the developing flow-eddy diffusivity model.

Assumption of a boundary layer of $y^+ = 4.3$ and an average velocity for the boundary layer of $u^* = 2.15$ with the fluctuation frequency from Equation (12) yields a

Table 3. Experimental Turbulent Peclet Numbers

Reference	Reynolds number	Turbulent Peclet number
Baldwin and Walsh	220,000-480,000	890-1000
Becker, Rosensweig, and Gwozdz	481,000-684,000	852
Towle and Sherwood	24,000-118,000	630-850
Flint	10,000- 86,000	870-1550
Mickelson	170,000-270,000	800-1200
Goldman and Marchello (He)	11,000- 23,000	1050-1500
Goldman and Marchello (CO_2)	12,000- 25,000	320-570
Goldman and Marchello (C_8H_{18})	11,000- 25,000	190-350

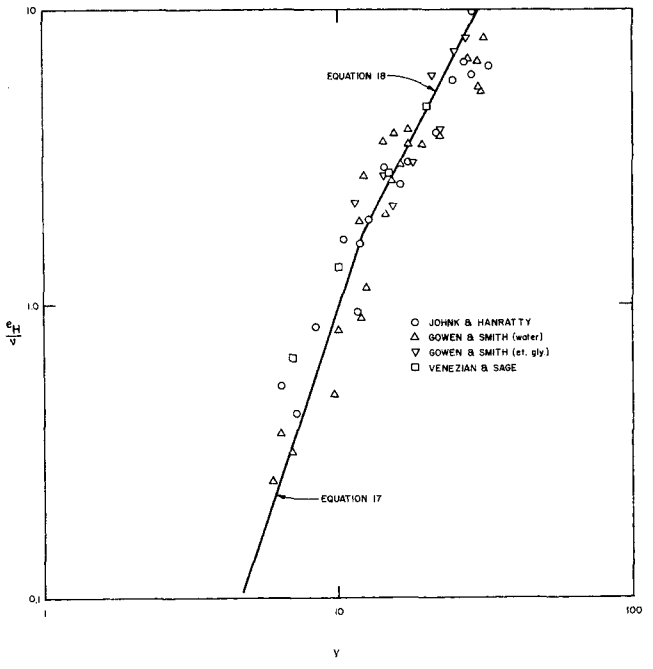

Fig. 2. Eddy diffusivity for the transition region.

distance that the laminar layer travels between fluctuations

$$x = 236\,\frac{\nu}{u^*} \tag{13}$$

Howarth (*28*) presents the reduced velocity u/U_∞ for the boundary layer along a flat plate at zero incidence as a function of the dimensionless distance from the plate, $\eta = y\sqrt{U_\infty/\nu x}$. Substitution of $y = y^+\,\nu/u^*$, x from Equation (13), and $U_\infty = 13\,u^*$ which corresponds to $y^+ = 35$ to obtain

$$\eta = y\sqrt{\frac{U_\infty}{\nu x}} = 0.235\,y^+$$

for turbulent pipe flow. The reduced velocity for the wall region of turbulent pipe flow can then be compared with the reduced velocity for a flat plate boundary layer at zero incidence. This comparison shows that the two profiles coincide from $y^+ = 0$ to $y^+ = 4.3$. The profiles diverge beyond $y^+ = 4.3$, with the turbulent flow velocity less than that for the boundary layer at zero incidence.

Heat and mass transfer relationships for the boundary layer in turbulent pipe flow can then be analyzed. Pohlhausen (*29*) derived the heat transfer equation for laminar flow on a plate at zero incidence as

$$N_{Nu} = 0.332\left(\frac{x\,U_\infty}{\nu}\right)^{1/2}(N_{Pr})^{1/3}$$

which can be expressed in mass transfer terms as

$$\frac{kx}{\mathcal{D}} = 0.332\left(\frac{x\,U_\infty}{\nu}\right)^{1/2}(N_{Sc})^{1/3} \tag{14}$$

Substitution of x from Equation (13) and $U_\infty = 13u^*$ yields

$$k = 0.078\,u^*\,N_{Sc}^{-2/3}$$

which is in excellent agreement with the equation obtained from the mass transfer data of Harriott and Hamilton (*30*)

$$k = 0.0816\,u^*\,N_{Sc}^{-2/3} \tag{15}$$

The comparison of the velocity profiles and the mass transfer analysis indicates similarity between turbulent pipe flow and a flat plate boundary layer at zero incidence. The pressure drop relationship is also of interest. Blasius (*31*) reported the dimensionless shearing stress for a flat plate

$$\frac{\tau_0\,g_c}{\rho\,U_\infty^2} = 0.332\sqrt{\frac{\nu}{U_\infty\,x}}$$

which leads to a friction factor-Reynolds number relationship

$$f' = \frac{0.664}{\sqrt{\dfrac{U_\infty\,x}{\nu}}}$$

Substitution of x from Equation (13) and $U_\infty = 13\,u^*$ yields

$$f' = 0.012$$

If pressure drop for turbulent pipe flow is defined by

$$\Delta P = \frac{4f'\,L\,U_\infty^2\,\rho}{2\,g_c\,D} \tag{16}$$

the friction factor of 0.012 is then applicable for the range of conditions that represent turbulent flow in a smooth pipe. This friction factor is observed to be equal to the Fanning friction factor at a Reynolds number DU/ν of 2100. Division of Equation (16) by the conventional equation for pressure drop yields the relationship between the two friction factors

$$\frac{f'}{f} = 0.012\left(\frac{U_\infty}{U}\right)^2$$

A Reynolds number $x\,u/\nu$ can be calculated as a function of y^+ for the laminar boundary layer with x from Equation (13). It is interesting to observe that this Reynolds number increases from zero at the wall to about 900 at $y^+ = 4.3$. This value is similar to the turbulent Peclet numbers shown in Table 3 for the core region of pipe flow. A Reynolds number $x\,u/(\epsilon + \nu)$ can also be estimated for the wall region in which eddy diffusion is a significant contribution. Equation (15) represents an eddy diffusivity relationship

$$\frac{\epsilon}{\nu} = 0.00096\,y^{+3} \tag{17}$$

Reynolds numbers calculated using Equations (13) and (17) are in the range of 900 to 1100 for the region $4.3 < y^+ < 12$. Thus, a critical Reynolds number appears to occur in this region.

The prior paper (*10*) also showed eddy diffusivities for

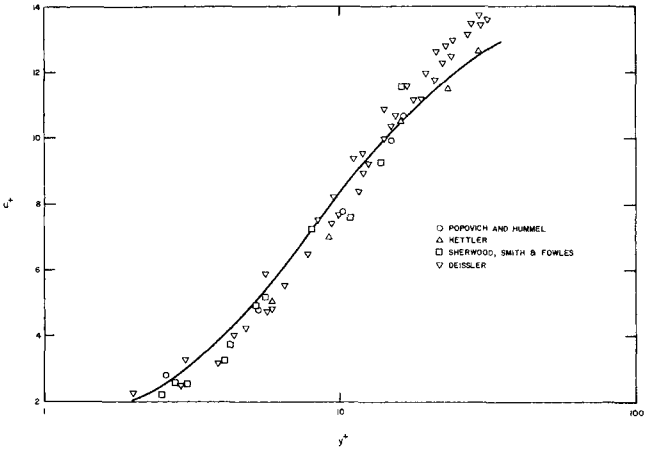

Fig. 3. Velocity profile.

heat from the temperature profile data of Johnk and Hanratty and Gowen and Smith. The smoothed diffusivity data of Venezian and Sage (32) for parallel plates were also shown. Figure 2 repeats these data with Equation (17) shown for $y^+ < 12$ and the equation

$$\frac{\epsilon_H}{\nu} = 0.0155\ y^{+\,1.9} \qquad (18)$$

for $12 < y^+ < 35$. It is observed that Equation (17) shows an excellent fit with the experimental data for heat transfer.

Equations (17) and (18) provide a test of the postulate that $\epsilon_\nu = \epsilon_H = \epsilon_m$ for the wall region. It is indicated that $\epsilon_H = \epsilon_m$ because Equation (17) is obtained from mass transfer data and is shown to fit ϵ_H data. Equations (17) and (18) can be assumed to represent eddy diffusivity for momentum to obtain a velocity profile from these equations. Figure 3 shows such a profile with experimental velocity data for comparison. The experimental data are those of Deissler (33) obtained by the hot-wire, Hettler (34), and Sherwood, Smith, and Fowles (35) by a particle method, and Popovich and Hummel by flash photolysis.

The agreement for the three methods is good for the region from the wall to about $y^+ = 12$, and it appears that the experimental velocities are less than the profile calculated from the eddy diffusivities for heat. At $y^+ > 15$ the hot-wire data show a higher velocity than the particle data, and the particle data show reasonable agreement with the profile calculated from the eddy diffusivities for heat. Thus, the comparison of the experimental velocity data with the calculated profile from the heat data does not present convincing proof that the eddy diffusivities for heat and momentum are equal in the wall region.

Figure 4 shows calculated values of k^+ for $0 < y^+ < 35$ as a function of the Prandtl and Schmidt numbers with Equations (17) and (18) and the numerical integration solution. The experimental heat transfer data of Friend and Metzner (36) and mass transfer data of Harriott and Hamilton (31) are shown to represent data with essentially all of the resistance in the $y^+ < 12$ region which corresponds to the Prandtl number range greater than 40. The heat transfer data of Bernardo and Eian (37), Dipprey and Sabersky (38), Eagle and Ferguson (39), and Hoffman (40) are shown for the Prandtl number range of 2.7 to 40. The heat transfer coefficient for the region $0 < y^+ < 35$ was calculated from the difference of the experimental coefficient and the coefficient estimated by numerical integration using the Bogue and Metzner equation for the $35 < y^+$ region with the assumption that ϵ_H and ϵ_ν are equal.

The resistance calculated for the core region represents a maximum of 15% of the total resistance for these data. Figure 4 shows also the heat transfer coefficients for the $y^+ < 35$ region calculated from the temperature profile data of Johnk and Hanratty for air, Gowen and Smith for water, and Buhr, Carr, and Balzhiser for the NaK eutectic. From Figure 4 it is observed that Equation (16) represents the transfer coefficients for Prandtl and Schmidt numbers greater than 3 and Equation (19) for the region from 0.02 to 3.

$$k^+ = e^{[-2.528\ -\ 0.6835 \ln N_{Pr}\ +\ 0.0285\ (N_{Pr})^2]} \qquad (19)$$

HEAT TRANSFER IN THE CORE REGION

Figure 5 shows the transfer coefficients for the core region ($y^+ > 35$) estimated from the experimental data of

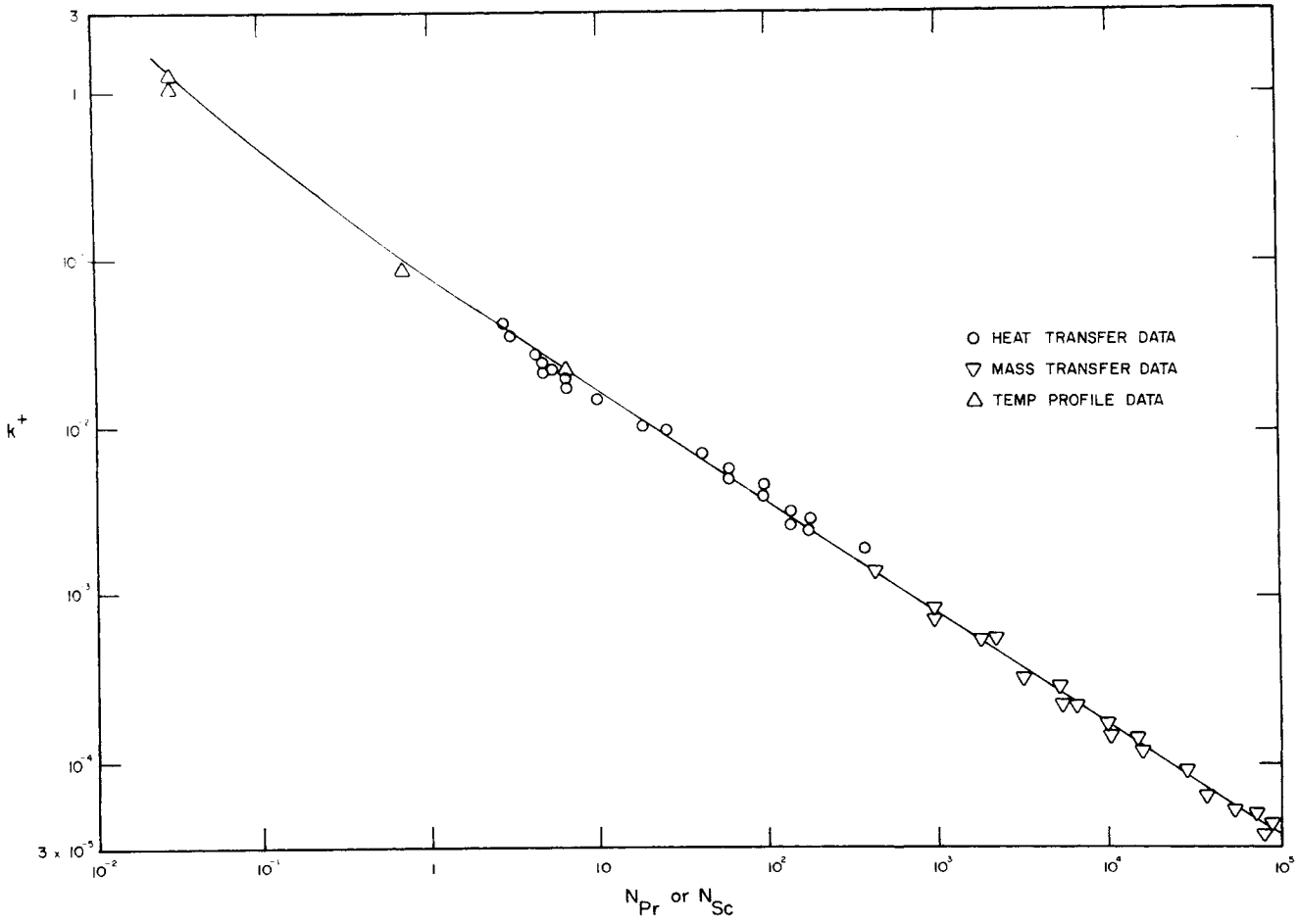

Fig. 4. Wall region dimensionless coefficient.

Buhr, Carr, and Balzhiser and of Talanov and Ushakov (*41*) for the NaK eutectic, Dipprey and Sabersky for water, and Kolar (*42*) for air. The estimated experimental coefficients for the core are the difference between the experimental coefficients and the coefficients for the wall region estimated from Figure 4. The maximum resistance of the wall region is about 20% of the total resistance for these data.

A comparison is shown with the transfer coefficients calculated for the core region by numerical integration using the Bogue and Metzner equation with the assumption that ϵ_H and ϵ_ν are equal. The calculated coefficients are observed to average about 20% higher than the estimated experimental coefficients. This is an indication that the assumption of equality of ϵ_H and ϵ_ν is reasonable even for Prandtl numbers of the order of 0.02. The consistent error shown by Figure 5 may be attributed, at least to some extent, to error in the estimation of ϵ_ν from the Bogue and Metzner equation for the velocity profile. It has been shown earlier in this paper by comparison of Tables 2 and 3 that the turbulent Peclet numbers calculated from the Bogue and Metzner equation indicate that the calculated eddy diffusivity is higher than the values obtained from the best of the experimental core data.

Heat transfer in the core region is a function of both eddy and molecular diffusion. Heat transfer coefficients for the region $y^+ > 35$ were calculated by the numerical solution for a range of molecular diffusivities using the Bogue and Metzner equation for the velocity profile. The relationship for these calculated heat transfer coefficients and the molecular thermal diffusivity was

$$\frac{k_M R_{35}}{K} = 3.58 \qquad (20)$$

If the total heat transfer coefficient for the core region is assumed to be the sum of the coefficients corresponding to molecular and eddy diffusion, the core heat transfer coefficient is then

$$k_T = k_M + k_{EC} \qquad (21)$$

Equation (21) was applied to the heat transfer data shown by Figure 5 to obtain values of k_{EC} from the experimental data. As dimensionless coefficients, these are found

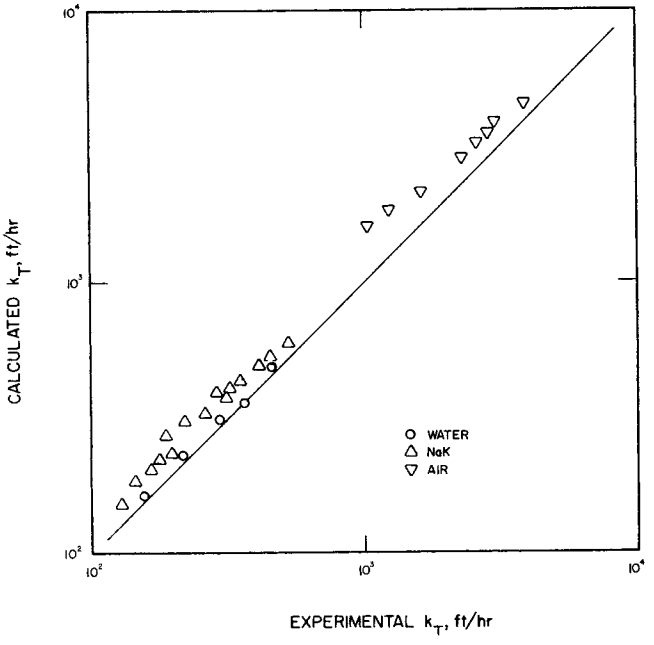

Fig. 5. Core heat transfer coefficient comparison.

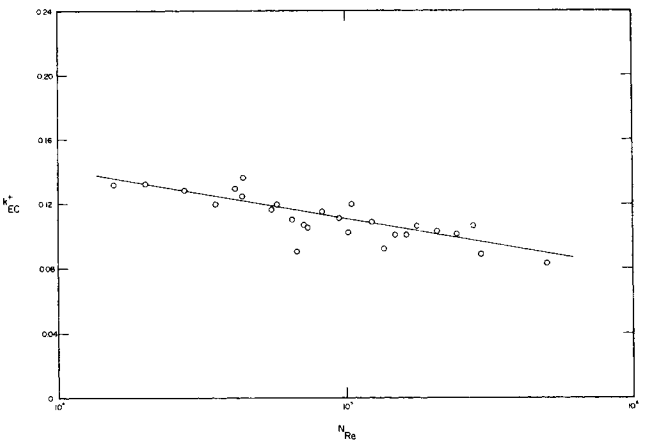

Fig. 6. Core heat transfer coefficients for eddy diffusion.

to be a function of Reynolds number as shown by Figure 6 and are represented by

$$k^+_{EC} = 0.264 - 0.0133 \ln N_{Re} \qquad (22)$$

HEAT AND MASS TRANSFER MODEL

Results of the analyses for the core and wall regions can be combined to provide a model for heat and mass transfer coefficients for turbulent flow in a smooth pipe. A coefficient for the wall region ($y^+ < 35$) is obtained as a function of the Prandtl or Schmidt number as shown by Figure 4. Equation (16) is observed to apply for Prandtl and Schmidt numbers greater than 3 and Equation (19) is an empirical representation of the data for Prandtl numbers in the range of 0.02 to 3. A coefficient for the core region ($y^+ > 35$) is obtained from combination of Equations (20), (21), and (22) to represent molecular and eddy diffusion. A resistance combination of these coefficients then represents the heat or mass transfer coefficient for turbulent flow in a smooth pipe.

This model differs from the model represented by Equation (1) because the wall region, with characteristics of laminar flow, is considered separately from the fully turbulent core region. Thus, this model has the capacity to apply for the Prandtl-Schmidt number range of 0.02 to 100,000, which is the range of the existing experimental data. Equation (1) is restricted to a limited range in which the wall region is the controlling contribution to heat or mass transfer.

DRAG REDUCING SYSTEMS

Many studies have been undertaken with regard to the physical aspects of drag reduction. The relationship between reduction in drag and reduction in the heat transfer coefficient has been of particular interest because this provides a rigorous test of the semitheoretical correlations for heat transfer which are based upon the friction factor. The experimental work reported by Gupta, Metzner, and Hartnett (*43*) for a 0.745-in.-diam. pipe are representative of drag and heat transfer data for viscoelastic fluids. Comparison with the Friend and Metzner (*44*) equation

$$N_{Nu} = \frac{(f/2)(C_p \rho v D/k)}{1.2 + 11.8 (f/2)^{1/2} (N_{Pr} - 1)(N_{Pr})^{-1/3}} \qquad (23)$$

is of particular interest because this equation has been found to apply for the Prandtl number range of 0.5 to 590 for Newtonian fluids and to "Power-law" non-Newtonian fluids (*44*). Lower values of the friction factor indicate

lower heat transfer coefficients from Equation (23), but the reduction in the heat transfer rate should be less than the reduction in drag as shown by this equation. The Gupta, Metzner, and Hartnett paper gives the comparison for experimental data shown in Table 3 for 0.05 wt. % ET 597 in water.

The paper also reports consideration of the ratio of the mean-to-maximum temperature difference and the ratio of maximum-to-mean velocity terms that are represented by constants for Newtonian turbulent flow in Equation (23). No realistic variation in these terms can account for the reduction in the heat transfer rate.

The velocity profile analysis used for Newtonian fluid heat transfer represents another approach to the drag-heat transfer relationship for viscoelastic fluids. Seyer and Metzner (*45*) report velocity profile data for 0.1 wt. % ET 597 in water for a 1-in. pipe. Velocity data were obtained from photographs of very small air bubbles in the fluid. This technique was used because impact and hot-wire methods have been questioned for turbulence research with viscoelastic fluids. Figure 7 shows the profile data obtained at average velocities of 10 and 19.2 ft./sec. The dimensionless radial distance for power law fluids is defined as

$$(y^+)^{1/\bar{n}} = \frac{yu^*\rho}{\mu_{aw}}$$

$$\mu_{aw} = \tau_0 g_c / (\tau_0/\bar{K})^{1/\bar{n}}$$

The velocity profile for Newtonian fluids is also shown and a thicker boundary layer is observed for the viscoelastic fluid. A boundary layer analysis can be used to estimate the eddy diffusivity for this case.

The Hanratty (*46*) analysis for the wall region based upon the turbulent exchange of mass and momentum with the wall yields

$$\frac{n\nu}{u^{*2}} = \frac{\pi}{4(u_L^+)^2} \qquad (24)$$

Solution of Equations (12) and (24) results in $u_L^+ = 9.3$ which corresponds to $y^+ \approx 12$. This indicates that the source of the fluctuations is y^+ of approximately 12 for Newtonian flow in a smooth pipe. Popovich and Hummel observed that flow is only occasionally turbulent in the region $y^+ < 12$. Thus, the frequency data indicate that the fluid masses moving against the wall possess a velocity corresponding to the limit of the "occasionally turbulent" region. The velocity profile for the viscoelastic fluid indicates that the "occasionally turbulent" region extends to

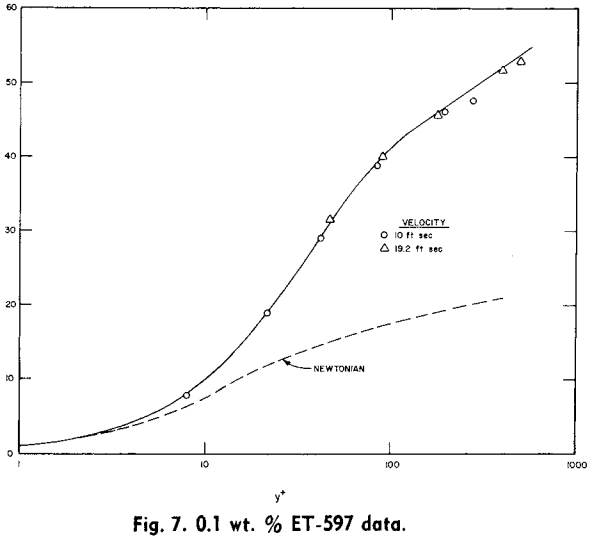

Fig. 7. 0.1 wt. % ET-597 data.

Table 4. Comparison of Reductions in Drag and Heat Transfer Rates

Flow rate (lb./min.)	Drag reduction (%)	Heat transfer rate reduction (%)
100	22	58
200	44	62

$y^+ \approx 40$ and $u_L^+ = 28$. Substitution in Equation (24) shows

$$\frac{n\nu}{u^{*2}} = 1 \times 10^{-3}$$

Assumption of a boundary layer of $y^+ = 7$ and an average boundary layer velocity of 3.5 u^* results in

$$x = 3500 \frac{\nu}{u^*}$$

Substitution in Equation (14) of this value of x and $U_\infty = 41u^*$ corresponding to $y^+ = 100$ for the viscoelastic fluid provides

$$k = 0.0336\ u^*\ (N_{Sc})^{-2/3}$$

and

$$\frac{\epsilon}{\nu} = 0.000067\ y^{+3} \qquad (25)$$

Comparison of Equations (17) and (25) indicates that the eddy diffusivity near the wall is about 7% of that for a Newtonian fluid. Numerical integration using the velocity profile from Figure 7 with $\epsilon_H = \epsilon_\nu$ for $y^+ > 40$ and Equation (25) for $y^+ < 40$ shows that the heat transfer coefficient is 10% of that for water at a velocity of 10 ft./sec. and the drag is 39% of that for water at this velocity. The numerical integration also provides a check on the average velocity from the integrated profile. For this case, the value was 9.85 ft./sec. which is excellent agreement with the actual velocity of 10 ft./sec. Experimental heat transfer data are not available for this flow rate of 0.1 wt % ET 597 in a 1-in. pipe, so there is no check on the calculated heat transfer rate. Comparison with the data in Table 4 shows a heat transfer reduction much greater than the drag reduction, and at least the calculated heat transfer rate shows the same result.

SUMMARY

Analysis of temperature profile data for the turbulent core indicates that the ratio of the eddy diffusivities of heat and momentum are approximately unity for data with the Prandtl number range of 0.029 to 14.3. Temperature profile data for the wall region show that eddy diffusivity for heat data in the range $5 < y^+ < 12$ are consistent with the eddy diffusivity for mass relationship obtained from mass transfer data at high Schmidt numbers. This relationship is also approximated by a model for developing flow in the laminar sublayer with a fluctuation frequency reported by Sirkar and Hanratty. Numerical integration of the velocity profile with the wall region eddy diffusivity relationships provides heat transfer coefficients for constant heat flux that are in good agreement with experimental data for this region.

Calculation of heat transfer coefficients by numerical integration with the Bogue and Metzner equation for the core velocity profile wih $\epsilon_H = \epsilon_\nu$ results in coefficients that are about 20% higher than experimental values. Equations are developed for dimensionless coefficients for the wall region and for the core to provide a model for heat and

mass transfer for the Prandtl-Schmidt number range of 0.02 to 100,000. Estimation of the heat transfer coefficient from the velocity profile for a viscoelastic fluid shows a greater reduction in heat transfer rate than in drag. This is consistent with experimental observations.

NOTATION

a = pipe radius, ft.
D = pipe diameter, ft.
f = Fanning friction factor
f' = friction factor for Equation (16)
g_c = conversion constant, ft. lb. mass/lb. force/hr.^{2}
K = thermal diffusivity, sq.ft./hr.
$\overline{K}$ = consistency index, lb. mass hr.$^{\overline{n}}$/sq.ft.
k = mass transfer or heat transfer coefficient, ft./hr.
k^+ = dimensionless mass transfer or heat transfer coefficient, k_E/u^*
N_{Nu} = Nusselt number
N_{Pe} = Peclet number
N_{Pr} = Prandtl number
N_{Re} = Reynolds number
N_{Sc} = Schmidt number
n = frequency, hr.$^{-1}$
$\overline{n}$ = flow behavior index, dimensionless
ΔP = pressure drop for pipe
R_{35} = pipe radius from centerline to $y^+ = 35$, ft.
r = radial distance from pipe center line, ft.
U = mean velocity
U_∞ = free stream velocity, velocity at $y^+ = 35$ for Newtonian turbulent pipe flow
u = velocity in axial direction, ft./hr.
$u_L{}^+$ = dimensionless velocity in axial direction of fluid mass before contact with the wall, ft./hr.
u^+ = u/u^*
u^* = $\sqrt{\tau_0 g_c/\rho}$, ft./hr.
x = distance from leading edge of plate
y = perpendicular distance from wall, ft.
y^+ = $y\,u^*/\nu$

Greek Letters

ϵ = eddy diffusivity, sq.ft./hr.
μ = fluid viscosity, lb. mass/ft.hr.
μ_{aw} = apparent viscosity evaluated at wall shear stress, lb. mass/ft.hr.
η = dimensionless distance from wall, $y\sqrt{U_\infty/\nu x}$
ν = kinematic viscosity, μ/ρ, sq.ft./hr.
ξ = y/a
ρ = fluid density, lb. mass/cu.ft.
τ_0 = shear stress at wall, lb. force/sq.ft.

Subscripts

c = center line
E = experimental
EC = eddy diffusion, core
H = heat
M = molecular diffusion
m = mass
T = total core
ν = momentum

LITERATURE CITED

1. Colburn, A. P., *Trans. Am. Inst. Chem. Engrs.*, **29**, 174 (1933).
2. Dittus, P. W., and L. M. K. Boelter, *Univ. of Calif. Eng. Pub.*, **2**, 443 (1930).
3. Drexel, R. E., and W. H. McAdams, *Natl. Advisory Comm. Aeron., ARR* No. 4F28 (1945).
4. Sieder, E. N., and G. E. Tate, *Ind. Eng. Chem.*, **28**, 1429 (1936).
5. von Karman, T., *Trans. Am. Soc. Mech. Engrs.*, **61**, 705 (1939).
6. Nikuradse, J., *VDI-Forschungsh.*, **356**, 1 (1932).
7. Martinelli, R. C., *Trans. Am. Soc. Mech. Engrs.*, **69**, 947 (1947).
8. Lin, C. S., R. W. Moulton, and G. L. Putnam, *Ind. Eng. Chem.*, **45**, 636 (1953).
9. Kropholler, H. W., and A. D. Carr, *Intern. J. Heat Mass Transfer*, **5**, 1191 (1962).
10. Hughmark, G. A., *Ind. Eng. Chem. Fundamentals*, **8**, 31 (1969).
11. Jenkins, R., "1951 Heat Transfer and Fluid Mechanics Institute," Stanford University Press, Palo Alto, Calif. (1951).
12. Azer, N. Z., and B. T. Chao, *Intern. J. Heat Mass Transfer*, **1**, 121 (1960).
13. Deissler, R. G., *ibid.*, **6**, 257 (1963).
14. Tyldesley, J. R., and R. S. Silver, *ibid.*, **11**, 1325 (1968).
15. Goldman, I. B., and J. M. Marchello, *ibid.*, **12**, 797 (1969).
16. Baldwin, L. V., and T. J. Walsh, *AIChE J.*, **7**, 53 (1961).
17. Johnk, R. E., and T. J. Hanratty, *Chem. Eng. Sci.*, **17**, 867 (1962).
18. Bogue, D. C., and A. B. Metzner, *Ind. Eng. Chem. Fundamentals*, **2**, 143 (1963).
19. Buhr, H. O., A. D. Carr, and R. E. Balzhiser, *Intern. J. Heat Mass Transfer*, **11**, 641 (1968).
20. Gowen, R. A., and J. W. Smith, *Chem. Eng. Sci.*, **22**, 1701 (1967).
21. Becker, H. A., R. E. Rosensweig, and J. B. Gwozdz, *AIChE J.*, **12**, 964 (1966).
22. Towle, W. L., and T. K. Sherwood, *Ind. Eng. Chem.*, **31**, 457 (1939).
23. Flint, D. L., Hisao Kada, and T. J. Hanratty, *AIChE J.*, **6**, 325 (1960).
24. Mickelsen, W. R., Natl. Advisory Comm. Aeronaut. Tech. Note 3570 (1955).
25. Hughmark, G. A., *AIChE J.*, **17**, 51 (1971).
26. Sirkar, K. K., and T. J. Hanratty, paper presented at AIChE meeting, Washington, D. C. (Nov. 1969).
27. Popovich, A. T., and R. L. Hummel, *AIChE J.*, **13**, 854 (1967).
28. Howarth, L., *Proc. Roy. Soc., London, A.*, 164, 547 (1938).
29. Pohlhausen, E., *Angew. Math. Mech.*, **1**, 115 (1921).
30. Harriott, P., and R. M. Hamilton, *Chem. Eng. Sci.*, **20**, 1073 (1965).
31. Blasius, H., *Z. Math. U. Phys.*, **56**, 1 (1908).
32. Venezian, E., and B. H. Sage, *AIChE J.*, **4**, 393 (1958).
33. Deissler, R. G., *Natl. Advisory Comm. Aeron., Tech. Note*, 2138 (1950).
34. Hettler, J. P., P. Muntzer, and O. Scrivener, *Compt. Rend.*, **258**, 4201 (1964).
35. Sherwood, T. K., K. A. Smith, and P. E. Fowles, *Chem. Eng. Sci.*, **23**, 1225 (1968).
36. Friend, W. L., and A. B. Metzner, *AIChE J.*, **4**, 393 (1958).
37. Bernardo, Everett, and C. S. Eian, *Natl. Advisory Comm. Aeron. ARR* No. E5F07 (1945).
38. Dipprey, D. F., and R. H. Sabersky, *Intern. J. Heat Mass Transfer*, **6**, 329 (1963).
39. Eagle, Albert, and R. M. Ferguson, *Proc. Roy. Soc. London*, **A127**, 540 (1930).
40. Hoffman, H. W., "1953 Heat Transfer and Fluid Mechanics Institute," p. 83, Stanford University Press, Stanford, Calif. (1953).
41. Talanov, V. D., and P. A. Ushakov, *Liquid Metals Atomizdat*, 9, Moscow (1967); translated NASA TT F-22 (May, 1969).
42. Kolar, V., *Intern. J. Heat Mass Transfer*, **8**, 639 (1965).
43. Gupta, M. K., A. B. Metzner, and J. P. Hartnett, *ibid.*, **10**, 1211 (1967).
44. Friend, P. S., and A. B. Metzner, *Ind. Eng. Chem.*, **51**, 879 (1959).
45. Seyer, F. A., and A. B. Metzner, *AIChE J.*, **15**, 426 (1969).
46. Hanratty, T. J., *AIChE J.*, **2**, 359 (1956).

Manuscript received March 25, 1970; revision received June 3, 1970; paper accepted June 7, 1970.